Deflated regime for pressurized ring polymers with long-range interactions

U. Marini Bettolo Marconi
Dipartimento di Matematica e Fisica, Università degli Studi di Camerino, via Madonna delle Carceri, 62032 Carmerino, Italy

A. Maritan
Dipartimento di Fisica, Università degli Studi di Padova and Istituto Nazionale di Fisica Nucleare, Sezione di Padova, via F. Marzolo 8, 35131 Padova, Italy

(Received 22 October 1992)

Two-dimensional vesicles subject to osmotic pressure imbalance may be modeled as unrestricted random rings. Assuming a pressure that couples to the square of the oriented area we are able to obtain an exactly solvable model that accommodates the deflated regime corresponding to a shriveled vesicle. Moreover, we investigated the effects of a long-range repulsive, nonlocal interaction among monomers by employing a variational approach. We find good agreement between our analytical predictions and Monte Carlo simulation results.

PACS number(s): 87.15.He, 05.40.+j

Recently there has been considerable interest in understanding the behavior of vesicles [1] as a prototype of more general systems such as interfaces, membranes, and random surface [2,3]. Real vesicles, e.g., red blood cells, exhibit a variety of well-defined but fluctuating shapes [4].

Even in two dimensions the behavior is very rich, characterized by continuously variable fractal shapes, several universalities classes, including self-avoiding walks and branched polymers, and a dynamical phenomena such as flicker. An internal pressure increment δp acts on the vesicle controlling the internal area of the vesicle. When $\delta p > 0$ the vesicle becomes circular. On the much richer deflated regime ($\delta p < 0$), numerical simulations have suggested that the vesicles collapse to form a branched polymer [1,5–7].

Recently, Rudnick and Gaspari (RG) [8] introduced a simple exactly solvable model for the study of vesicles in the inflated regime ($\delta p > 0$). Omitting excluded volume effects, they consider a pressure that favors an oriented area, thus excluding the possible study of the deflated regime. Our focus is on modifying their approach to make this interesting regime accessible. Specifically, employing a pressure that couples to the square of the algebraic area (or its modulus), we obtain an analytically tractable model that yields the scaling behavior in the deflated regime exactly. As we checked numerically, this choice, although dictated by mathematical convenience, does not alter the asymptotic behavior that one would observe in the presence of a pressure coupled to the modulus of the oriented area. Further, the effects of the long-range repulsive interactions are treated variationally leading to nonuniversal behavior. Monte Carlo simulations have been carried out to confirm the prediction.

The model is described by the following Hamiltonian:

$$H=\alpha \sum_{i=1}^{N} (\mathbf{R}_{i+1}-\mathbf{R}_i)^2+\tfrac{1}{2} \sum_{i,j=1}^{N}{}' U((\mathbf{R}_i-\mathbf{R}_j)^2)+V_{\text{area}} , \tag{1}$$

where $U(x)\sim x^{-\lambda/2}$ for large x is the long-range two-body interaction acting among the nodes of the ring placed at positions $\mathbf{R}_i$ (with the cyclic condition $\mathbf{R}_i=\mathbf{R}_{i+N}$), and $i=1,2,\ldots,N$. The prime in the second sum means that $i=j$ is excluded. Long-range forces have been introduced in the context of critical phenomena for a vector spin model in Ref. [9]. Our case corresponds to the zero component limit, when the pressure is absent [10]. Moreover, the excluded-volume interaction $\delta^d(\mathbf{R}_i-\mathbf{R}_j)$ corresponds to the choice $\lambda=d$, as discussed in Ref. [11], whereas $\lambda=-2$ to the Gaussian case.

The first term in Eq. (1) is the standard elastic energy [12] while the last term represents the energy contribution coming from the pressure imbalance. Equation (1) reduces to the RG case in the absence of the long-range potential with $V_{\text{area}}=pA$, and the algebraic area A given by

$$A=\hat{\mathbf{z}}\cdot\Big(\sum_{i=1}^{N} \mathbf{R}_{i+1}\times\mathbf{R}_i\Big) , \tag{2}$$

where $\mathbf{R}_i$ lie in the xy plane and $\hat{\mathbf{z}}$ is the unit normal to the plane. Independent of the sign of p, this model favors inflated configurations and it is characterized by an instability for $|p|>p_c$ [8].

In order to analyze the interesting deflated regime of the vesicle we have considered the two cases

$$\begin{aligned} V_{\text{area}} &= pA^2 \\ &= p|A| . \end{aligned} \tag{3}$$

The first case can be solved exactly when long-range forces are absent, whereas the second cannot. Although the latter case is closer to physical reality [1,6], our variational calculations indicate no substantial qualitative difference. We will therefore present details only for the former.

In the absence of long-range interactions using the Hubbard-Stratonovich transformation we can rewrite the partition function as

$$Z_t=\frac{1}{\sqrt{4\pi|p|}}\int dg e^{-g^2/4|p|}\int d[\mathbf{R}]e^{-H_0}\ , \tag{4}$$

where H_0 contains the elastic term and $V_{\rm area}$ is now igA. $d[\mathbf{R}]$ indicates the integration over all $\mathbf{R}_i$'s with the constraint that the center of mass is fixed at the origin and k_BT has been adsorbed in the coupling constants. Since H_0 is quadratic, the integration over the $\mathbf{R}_i$'s can be easily done, while the integration over g is done using saddle point, yielding for the free-energy density

$$f=-\frac{\ln Z}{N}$$
$$=\frac{\ln p}{2N}+\min_g\left[\frac{g^2}{4|p|N}+\frac{2}{2N}\sum_k\ln|c_k^2+4g^2\sin^2k|\right], \tag{5}$$

where an irrelevant constant has been omitted, $c_k=4\alpha(1-\cos k)$ and $k=2\pi n/N$ with $n=1,2,\ldots,(N-1)$.

The minimum in Eq. (5) occurs at $g=0$. The leading order in the asymptotic behavior of the averaged squared area and radius of gyration R^2 is obtained by saddle-point corrections in Eq. (4) expanding about $k=0$ and extending the sum over $n=Nk/2\pi$ to $n=\infty$. The results are

$$\langle A^2\rangle=-\frac{\partial\ln Z}{\partial p}=\frac{\langle A^2\rangle_{p=0}}{1+2p\langle A^2\rangle_{p=0}} \tag{6}$$

and

$$\langle R^2\rangle=\frac{1}{2N^2}\sum_{i,j}\langle(\mathbf{R}_i-\mathbf{R}_j)^2\rangle$$
$$=\frac{3}{b^2}[b\coth(b)-1]\langle R^2\rangle_{p=0}\ , \tag{7}$$

where

$$\langle A^2\rangle_{p=0}=24\langle R^2\rangle_{p=0}^2\ , \tag{8}$$

$$\langle R^2\rangle_{p=0}=\frac{N^{2\nu}}{24\alpha}\ , \tag{9}$$

and $\nu=\frac{1}{2}$, $b=(\alpha^2/2N^2p+1/24)^{-1/2}$.

Thus the radius of gyration is almost insensitive to the "pressure," whereas the area fluctuations are finite when p is fixed [see Eq. (6)]. On the other hand, $\langle A^2\rangle\sim\langle R^2\rangle^2$ where $p=0$. When self-intersections are forbidden, the area $\langle A\rangle$ is proportional to the radius of gyration [1,5,6], but as soon as $p>0$ the universality class changes, $\langle A\rangle\sim N$ and $\langle R^2\rangle\sim N^{2\nu}$, where $\nu=0.64$ is the branched polymer ν exponent [1,6].

We now consider the long-range interaction U. It is known [11,13] that in the absence of pressure imbalance, the Hartree approximation predicts a nontrivial asymptotic behavior for $\nu=\max(2/\lambda,2/d)$ in dimension d, where $2<\lambda<4$ and $d\le4$. It has been conjectured [13,14] that when $2<\lambda<4,d$, the result $\nu=2/\lambda$ is exact when this ratio exceeds the exponent corresponding to the short-range repulsion $\nu_{\rm SR}$. In $d=2$, $\nu_{\rm SR}=\frac{3}{4}$ [15], implying that $\nu=2/\lambda$ when $2<\lambda<\frac{8}{3}$. We have applied the Hartree approximation for λ within this range when $V_{\rm area}$ is present and compared our results with Monte Carlo simulations for the $\lambda=2.5$ case.

The Hartree or Gaussian variational approach is based on the well-known Gibbs inequality for the free energy $f\le f_t+\langle H-H_t\rangle_t/N$, where H_t is a trial Hamiltonian, $\langle\ \rangle_t$ indicates the thermal average performed with the Boltzmann weight $\exp(-H_t)$, and f_t is the corresponding free energy. In terms of the Fourier transform of $\mathbf{R}_i$'s defined as

$$\tilde{\mathbf{R}}_k=\frac{1}{\sqrt{N}}\sum_{j=1}^{N}e^{ikj}\mathbf{R}_j \tag{10}$$

($\tilde{\mathbf{R}}_0=\mathbf{0}$ since the center of mass is fixed at the origin), we choose

$$H_t=\tfrac{1}{2}\sum_k c_k\tilde{\mathbf{R}}_k\tilde{\mathbf{R}}_{-k}+V_{\rm area}\ , \tag{11}$$

i.e., a Gaussian trial Hamiltonian plus a pressure term. It is extremely important to retain the pressure term in the trial Hamiltonian in order to recover the exact answer in the $U\to0$ limit. The best choice of f is obtained by minimizing

$$f_H=f_t+\frac{1}{N}\langle H-H_t\rangle_t \tag{12}$$

with respect to the c_k's where f_t is given by Eq. (5) and the second term in Eq. (12) is given by

$$\frac{1}{N}\langle H-H_t\rangle_t=\sum_k[4\alpha(1-\cos k)-c_k]\frac{\partial f_t}{\partial c_k}$$
$$+\tfrac{1}{2}\sum_{\substack{i,j\\ i\neq j}}\langle U[(\mathbf{R}_i-\mathbf{R}_j)^2]\rangle_t\ . \tag{13}$$

Here, we have made use of the identity

$$\frac{1}{N}\langle\tilde{\mathbf{R}}_k\tilde{\mathbf{R}}_{-k}\rangle_t=2\frac{\partial f_t}{\partial c_k}\ .$$

In order to evaluate the last term in Eq. (13) it is convenient to introduce the probability density for $(\mathbf{R}_i-\mathbf{R}_j)$, $P_{ij}(\mathbf{R})=\langle\delta^{(2)}(\mathbf{R}-\mathbf{R}_i+\mathbf{R}_j)\rangle_t$. Since the minimum in Eq. (5) occurs at $g=0$, within the saddle-point approximation, using the Fourier representation for the δ function, we easily find

$$P_{ij}(\mathbf{R})=(2\pi\Delta_{i-j})^{-1}e^{-(R^2/2\Delta_{i-j})}\ , \tag{14a}$$

where

$$\Delta_j=\tfrac{1}{2}\langle(\mathbf{R}_0-\mathbf{R}_j)^2\rangle=2\sum_k[1-\cos(kj)]\frac{1}{c_k}\ . \tag{14b}$$

Thus we obtain the following expression for the last term in Eq. (13):

$$\tfrac{1}{2}\sum_{\substack{i,j\\ i\neq j}}\langle U((\mathbf{R}_i-\mathbf{R}_j)^2)\rangle_t=\tfrac{1}{2}\sum_j\hat{\mathbf{U}}(\Delta_j) \tag{15}$$

with the definition

$$\hat{U}(\Delta_j)=\int d^2R P_{i,j+i}(\mathbf{R})U(\mathbf{R}^2)$$
$$=\int_0^\infty dx\, e^{-x}U(2\Delta_j x)\ . \tag{16}$$

Using Eqs. (12)–(16) the variational equation $\partial f_H/\partial c_k=0$ is equivalent to the self-consistent equation:

$$c_k=4\alpha(1-\cos k)+\sum_j[1-\cos(kj)]\frac{\partial\hat{U}(\Delta_j)}{\partial\Delta_j} \tag{17}$$

(see also Sec. IV of [11]). Before discussing the solution of Eq. (17), let us calculate the averages of squared area and radius of gyration. From the relation $\langle A^2\rangle=\partial(Nf_H)/\partial p$ and from the definition (7) of $\langle R^2\rangle$ we get again

$$\langle A^2\rangle=\frac{\langle A^2\rangle_{p=0}}{1+2p\langle A^2\rangle_{p=0}}\ , \tag{18a}$$

as in Eq. (6), but with

$$\langle A^2\rangle_{p=0}=4\sum_k\frac{\sin^2 k}{c_k^2} \tag{18b}$$

and

$$\langle R^2\rangle=\frac{2}{N}\sum_k\frac{c_k}{c_k^2+4\langle g^2\rangle\sin^2 k}\ , \tag{19}$$

where $\langle g^2\rangle=2p/(1+2p\langle A^2\rangle_{p=0})$ comes from the saddle-point approximation when N is large. In the absence of a long-range potential Eq. (17) gives the (obvious) exact result $c_k=4\alpha(1-\cos k)$, which inserted into Eqs. (18) and (19) reproduces the results (6)–(9). When $U(x)\sim x^{-\lambda/2}$ for $x\gg1$, Eq. (17) can be solved for the leading behaviors of c_k at low k, which is the one of interest for the large-scale behavior in Eqs. (18) and (19). The analysis in Ref. [11] readily applies to Eq. (17) giving

$$c_k\sim Ck^{2\nu+1},\quad \nu=2/\lambda\ , \tag{20}$$

and $\lambda>2$ (see also Ref. [11]). The constant C can be calculated from Eq. (17) using the ansatz (20), but its specific value is not of interest here (see, however, Ref. [11]). From Eq. (18b) one finally obtains

$$\langle A^2\rangle_{p=0}=A_0N^{4\nu}\ , \tag{21}$$

where $A_0=4\zeta(4\nu)/C^2(2\pi)^{4\nu}$ and ζ is the Riemann's function. Equation (19) gives

$$\langle R^2\rangle=N^{2\nu}G(p\langle A^2\rangle_{p=0})\ , \tag{22}$$

where $G(x)$ is a bounded function always of order $O(x^0)$. Thus at $p=0$ we again obtain that $\langle A^2\rangle_{p=0}\sim\langle R^2\rangle^2_{p=0}$, as in the absence of a long-range potential. We tested our findings by Monte Carlo simulations for several values of p and N and $\lambda=2.5$. The technique is quite standard [16] (see also [14]).

In Figs. 1(a) and 1(b) $\langle R^2\rangle N^{-2\nu}$ and $\langle A^2\rangle_{p=0}/\langle A^2\rangle_p$ are plotted versus the scaling variable $x=p\langle A^2\rangle_{p=0}$, respectively. The exponent ν, which we have used, has been obtained for $p=0$ and the best fit is shown in Fig. 2 with the result

$$\nu=0.8\pm0.05\ , \tag{23}$$

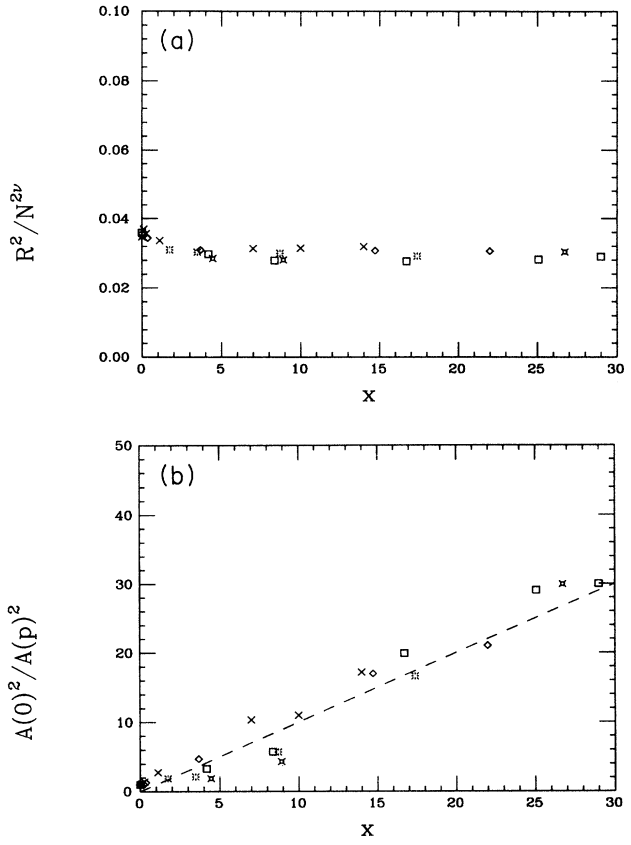

FIG. 1. (a) The reduced radius of gyration $\langle R^2\rangle N^{-2\nu}$ is plotted as a function of the scaling variable $x=p\langle A^2\rangle_{p=0}$ for the following cases: $N=10$ (crosses); $N=20$ (diamonds), $N=40$ (squares), $N=60$ (stars); $N=100$ (crosses with holes). (b) $\langle A^2\rangle_{p=0}/\langle A^2\rangle_p$ plotted vs the scaling variable x, for different choices of N as in (a). The dashed line represents the scaling function $(1+2x)$.

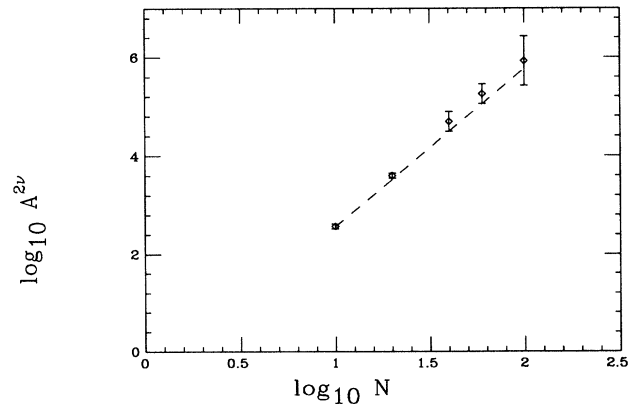

FIG. 2. Log-log plot of the quadratic area $\langle A^2\rangle$, calculated at $p=0$, against N. The dashed line shows the slope corresponding to the exponent $\nu=0.8$.

which must be compared with the variational estimate $\nu=2/\lambda=0.8$ of Eq. (20). The dashed line in Fig. 1(b) represents the scaling function $(1+2x)$ as we obtained from our variational calculation in Eq. (18a). The agreement is quite surprising in view of the rather simple approximations employed.

Better results may be obtained with a cleverer choice for the trial Hamiltonian than the one made in Eq. (11). In particular, one should take into account that even in the absence of a pressure term in Eq. (1), the long-range potential generates an effective pressure imbalance that one should incorporate in H_t.

In conclusion, we have introduced an alternative exactly solvable model for self-intersecting rings with a pressure imbalance coupled to the square of the algebraic area. This allows us to investigate the deflated regime, which was inaccessible to previous studies of related models [8], and there are no unphysical instabilities. The introduction of a long-range potential for monomer interaction is treated in the variational framework of the Hartree approximation as in Refs. [11] and [13]. Results from numerical simulations compare rather well with the analytical predictions and in particular the scaling variable $p\langle A^2\rangle_{p=0}$ turns out to be the correct choice. The radius of gyration is found to be insensitive to pressure imbalance and is universal in the entire $p>0$ region.

We have benefited from discussions with J. R. Banavar. We also thank him for a critical reading of the manuscript. A.M. was supported in part by the U.S. Office of Naval Research.

[1] S. Leibler, R. R. P. Singh, and M. E. Fisher, Phys. Rev. Lett. **59**, 1989 (1987); M. E. Fisher, Physica D **38**, 112 (1989), and references therein, C. J. Camacho and M. E. Fisher, Phys. Rev. Lett. **65**, 9 (1990).

[2] J. R. Banavar, A. Maritan, and A. L. Stella, Science **252**, 825 (1991).

[3] *Statistical Mechanics of Membranes and Surfaces,* edited by D. Nelson, T. Piran, and S. Weinberg (World Scientific, Singapore, 1987).

[4] F. Brochard and J. F. Lennon, J. Phys. (Paris) **36**, 1035 (1975).

[5] B. Duplantier, Phys. Rev. Lett. **64**, 493 (1990).

[6] J. R. Banavar, A. Maritan, and A. L. Stella, Phys. Rev. A **43**, 5752 (1991).

[7] M. Di Stasio, F. Seno, and A. L. Stella, J. Phys. A **25**, 3891 (1992).

[8] J. Rudnick and G. Gaspari, Science **252**, 422 (1991); E. Levinson, Phys. Rev. A **45** , 3629 (1992).

[9] A. Weinrib and B. I. Halperin Phys. Rev. B **27**, 413 (1983); M. E. Fisher, S. K. Ma, and B. G. Nickel, Phys. Rev. Lett. **29**, 917 (1972).

[10] P. G. de Gennes, *Scaling Concepts in Polymer Physics* (Cornell University Press, Ithaca, NY, 1979).

[11] J. des Cloizeaux, J. Phys. (Paris) **31**, 715 (1970).

[12] M. Doi and S. F. Edwards, *The Theory of Polymer Dynamics* (Oxford University Press, Oxford, 1986).

[13] J. P. Bouchaud, M. Mezard, G. Parisi, and J. S. Yedidia, J. Phys. A **24**, L1025 (1991).

[14] E. Marinari and G. Parisi, Europhys. Lett. **15**, 721 (1991).

[15] B. Nienhuis, Phys. Rev. Lett. **49**, 1062 (1982).

[16] See, e.g., K. Binder and D. Stauffer, in *Applications of the Monte Carlo Method to Statistical Physics,* edited by K. Binder, Topics in Current Physics Vol. 36 (Springer, New York, 1987.